Contract No.:

This manuscript has been authored by Battelle Savannah River Alliance (BSRA), LLC under Contract No. 89303321CEM000080 with the U.S. Department of Energy (DOE) Office of Environmental Management (EM).

Nanocomposite Materials for Accelerating Decarbonization

Simona E. Hunyadi Murph,[1,2] and Henry Sessions, Jr.[1]*

[1]Savannah River National Laboratory
Aiken, SC 29808

[2]University of Georgia,
Athens, Georgia 30602

*Corresponding author e-mail: Simona.Murph@srnl.doe.gov

Abstract

Decarbonization is demonstrated by catalytic conversion of CO_2 to fuel by means of exposure of cadmium selenide (CdSe) quantum dots - titania (TiO_2) nanophotocatalysts to sunlight illumination. The primary products resulted from this chemical reaction are methanol, carbon monoxide, and hydrogen after several hours of exposure to sun light. The overall CO_2 conversion efficiency of such quantum dot-titania nanostructures was compared with that of pure TiO_2 nanorod array photocatalyst. Data shows an improved conversion efficiency when composite quantum dot-titania nanostructures were used in comparison with titania nanophotocatalysts. It is postulated that this is due to the additional absorbance of visible light by the quantum dots and generation of additional charge separation at the CdSe-TiO_2 interfaces. The conversion efficiency of such an artificial photosynthesis process remains to be optimized for practical applications.

Keywords: nano-photocatalysts, decarbonization, CO_2 conversion, cadmium selenide-titania nanocatalysts

Introduction:

Decarbonization is arguably one of the most promising technologies that can address concerns related to global warming. [1] The efforts of reducing carbon intensity on the environment relies on the reduction of the greenhouse gas emissions produced by combustion of fossil fuels or capturing carbon from the atmosphere. [2] Hydrogen, as alternative sources of energy, is also attractive in addressing decarbonization goals due to its renewability, and sustainability. [3] Hydrogen has also a very high energy density per unit weight (three times more than gasoline) and burns faster than gasoline. Hydrogen is nonpolluting and the byproduct of a hydrogen fuel cells is purified water. [4]

Studies suggests that the largest contributors to carbon emissions are electricity and heat power generation sectors followed by the transportation industry. [5] However, almost every sector of our society, including energy production, agriculture, goods and services generate carbon dioxide.[6] A wide array of strategies have been employed to accelerate decarbonization goals, namely CO_2 sequestration, CO_2 storage and use, or conversion of CO_2 to useful chemicals. Conversion of CO_2 to useful chemicals could not only diminish reliance on fossil fuels but can also serve as a renewable and non-toxic mitigation strategy for achieving a circular economy. [1-5] As an added benefit, this conversion process utilizes the greenhouse gas CO_2 as a reactant making the process nearly CO_2 neutral.

The simplest way of describing CO_2 conversion is: $CO_2 + H_2O + h\nu$ (solar light) $\rightarrow CH_4 + O_2$ (Eq.1). However, CO_2 is thermodynamically stable (Gibbs free energy of 394 kJ/mol) requiring significant energy to overcome its thermodynamic and kinetic barriers needed to react. [7] This conversion can be, however, achieved with the help of suitable catalysts. While an extraordinary effort has been made by the scientific community toward developing efficient processes to convert CO_2 to useful chemicals, the field must address a series of challenges before achieving a carbon-neutral economy. For example, directly capturing and converting CO_2 into liquid solar fuels that can be also easily stored and easily manufactured at scale are of interest. [8] Moreover, cost-effective materials and components that are highly efficient at converting solar energy-to-chemical fuel are needed.

On the quest for development of highly efficient and cost-effective solar conversion devices, researchers have been exploring new material compositions and pioneering designs. The scientific literature has produced a great amount of experiment and theory on CO_2 conversion on metal oxides, semiconductor materials, or other catalyst classes. [9-11] Novel hetero-structures with tailored morphologies and crystallinities were developed with the goals of improving their photon-free electron generation rate or shifting the absorption band on catalyst materials. Yu et. al demonstrated that CO_2 is reduced to CO and O_2 using Pt/TiO_2 catalysts. [12] Du et al. reported photocatalytic reduction of CO_2 to methane, carbon monoxide and hydrogen by $MoS_2/CdS/TiO_2$ nanotube catalysts. [13] Unfortunately, most of the photocatalysts have a very narrow band edge absorbance and provide limited amount of free electrons and protons on the surface for such a reaction. [14] Thus, to improve the CO_2 conversion efficiency, the challenge that remains is related to design a better photocatalyst that can absorb a broader spectrum of sun light and efficiently generate electron-hole pairs for the above reaction.

Nevertheless, their limitations in terms of the requirement for UV excitation and/or generally low conversion efficiencies (0.5%) have become evident. This is because reduction of CO_2 to hydrocarbons is a complex multistep reaction involving shared intermediates and multiple reaction pathways:

$$CO_2 + 2e^- + 2H^+ \rightarrow CO + \tfrac{1}{2} O_2 \quad (2)$$

$H_2O + 2h^+ \rightarrow ½\ O_2 + 2H^+$ (3)
CO_2 (aq.) + $2H^+ + 2e^- \rightarrow HCOOH$ (4)
$HCOOH + 2H^+ + 2e^- \rightarrow HCHO + H_2O$ (5)
$HCHO + 2H+ + 2e^- \rightarrow CH_3OH$ (6)
$CH_3OH + 2H^+ + 2e- \rightarrow CH_4 + H_2O$ (7)

Titania has been considered the most appropriate candidate for photocatalytic processes due to its powerful oxidation capability, superior charge transport, and corrosion resistance. Additionally, TiO_2 is inexpensive, has reasonable activity, and is abundant. [15] The absorption of photons from natural light in photocatalytic materials generates electrons and holes which could drive energy conversion processes in the solar-driven photoreduction of CO_2 and/or water-splitting for hydrogen fuels. Despite these attributes, the efficiency of TiO_2 for photovoltaic and photocatalytic applications is severely limited by its large band gap (~3.2 eV) and rapid charge carrier recombination dynamics which means that titania can use less than approximately 1% of the solar spectrum. [16,17]

We have developed and amassed active titania based nanohybrid catalysts with a multifunctional, broadband electromagnetic response for efficient solar energy conversion of CO_2. Specifically, we engineered the bandgap of the TiO_2 photocatalytic materials with quantum dots (CdSe) sensitizers to maximize the reaction channels for the photocatalytic conversion. Photocatalytic conversion of CO_2 is monitored with an in-house designed chamber that allows evaluation of nanocatalysts for solar fuels applications. A gas chromatographic analysis shows that the primary product is carbon monoxide and hydrogen along with methanol after several hours' exposure to sun light.

Experimental Section:

Materials Fabrication and Characterization: The TiO_2 nanorod array was fabricated in a custom-built electron beam evaporation system as described before. [16,17] Quantum dots CdSe nanoparticles were grown onto substrates of TiO_2 glass or silicon pads (10mm x10 mm) by a citrate reduction approach. [18, 19] To 45 mL of water were added 0.05 g of sodium citrate (Aldrich) and 2 mL of 4 × 10-2 M cadmium perchlorate (Aldrich). The pH was adjusted to 9.0 with 0.1 M NaOH. After the solution had been bubbled with nitrogen for 10 min, 2 mL of 1 × 10-2 M N,N-dimethylselenourea (Aldrich) was added, and the mixture was heated in a conventional 900-W microwave oven for 50 s. All samples were characterized using electron microscopy analysis (transmission electron microscopy analysis and scanning electron microscopy (SEM), particle size distribution by dynamic light scattering (DLS), zeta potential (effective surface charge) analysis, and elemental composition by energy dispersive X-ray (EDS) mapping to elucidate their morphology, topography and composition. The nanoparticle's optical properties were evaluated by UV-Vis absorption spectroscopy and photoluminescence spectroscopy. Electronic absorption spectra were acquired with a CARY 500 Scan UV–vis spectrophotometer. Scanning electron microscopy analysis was conducted on a Hitachi 4800 instrument. Light scattering and zeta potential measurements were carried out on Brookhaven Zeta PALS instrument.

Photocatalytic Conversion: Photocatalytic conversion of CO_2 was monitored with an in-house designed solar-gas chambers equipped with gas inlet and outlet, optical window and sample stage holder that allowed evaluation of nanocatalysts for solar fuels applications. The type and amount of hydrocarbons and other gases generated through prolonged light-soaking was quantified by a gas-chromatograph. The retention time was measured from the time of injection to the time of maximum per deflection for the component being observed. The photocatalytic chamber used was

strategically selected, allowing a direct gas analysis with the micro gas-chromatograph, without the need of intermediary sampling steps. Approximately 1 cm^3 of gas was injected each time. Standard gases were used as control samples to accurately elucidate the peak composition. Each column was calibrated before running samples of interests. The quantitative analysis of the chromatograms produced was resolved by measuring the peak area (computer generated data) of eluted compounds. The peak area is proportional to the amount (moles) of compound eluted and was expressed as abundance throughout the manuscript.

Results and Discussions:

Efforts have been devoted to producing and sensitizing TiO_2 nanomaterials with nanoparticles that absorb light at lower photon energies, thus extending absorption into the visible light region of the spectrum. Coupling of pure TiO_2 with quantum dots (QDs), and noble metals (NPs) extends the adsorption of solar energy in visible region and generate more electron-hole pairs, due to the smaller band gap of those sensitizers. [15-17]

Quantum dots (QDs) are semiconductor nanoparticles that have a diameter in the 1-10 nm range, coincident with their respective excitonic Bohr radii. [18, 19] Semiconductor quantum dots exhibit quantization effects in photo-conversion devices and offer several unique and important properties that are advantageous: (a) absorption and emission spectra that can be tuned by varying size, shape, structure, or by adjusting the nature of adsorbates; (b) preparation, surface modification, and attachment through solution-based chemistries, which are cost-saving techniques and amenable for scale up; (c) QDs utilize multiple exciton generation and hot carriers, which can greatly improve the device applications. These materials are highly photoluminescent, resistant to photobleaching compared to organic fluorophores and their bandgap energies are exquisitely tunable with particle diameter, based on quantum confinement effects. CdSe possess bulk bandgap energies in the visible region of the electromagnetic spectrum; and the particle size in the 1-10 nm regimes tunes the bandgap energies, and thus light emission energies, to shorter wavelength compared to the bulk.

The TiO_2 nanorod arrays were fabricated by a physical vapor deposition approach as reported in earlier studies. [16,17] The as-prepared materials were annealed at different temperature to alter the crystalline structures of each component. This versatile method allows for controlled growth of ordered arrays of TiO_2 on solid supports which maximizes the surface area available for further reactions. Cadmium selenide nanoparticles were grown onto the ordered arrays of TiO_2 nanostructure supports by a solution chemistry method. (Figure 1a, b). The transmission electron microscopy image shows production of approximatively 5 nm in diameter of CdSe nanoparticles. The UV–vis spectra present a typical shoulder at around 500 nm while the emission spectra display the characteristic peak at approximately 580 nm (Figure 2b) which is in agreement with the size of the nanoparticles (5nm in diameter) and data reported earlier. [18, 19]

Consistent with the implications of UV–Vis spectra, particle size analysis shows that the average CdSe particle size was 7 nm (hydrodynamic radius) while the surface charge $\xi = -62 \pm 3$ mV. The negative surface charge is due to the adsorbed citrate on the CdSe surface. The CdSe nanoparticles as grown onto TiO_2 ordered arrays of nanostructures are shown in Figure 3. Scanning electron microscopy (SEM) images (Figure 3a) show that the CdSe quantum dots are distributed over the entire titania nanorod surface. The UV–vis spectra (Figure 3b) show the typical absorption peaks for TiO_2 around 350 nm. The shoulder peak at approximately 500 nm is attributed to the CdSe nanoparticles in agreement with the optical properties of CdSe nanoparticles generated in solution. Energy dispersive X-ray analysis (EDs) of the nanomaterials is performed to evaluate

nanomaterial composition with representative data presented in Figure 3c. The results reveal the presence of the main components, including Cd, Se, Ti and O. The results are in agreement with SEM and UV-Vis data and confirm once again the CdSe deposition on titania based ordered arrays of nanostructures.

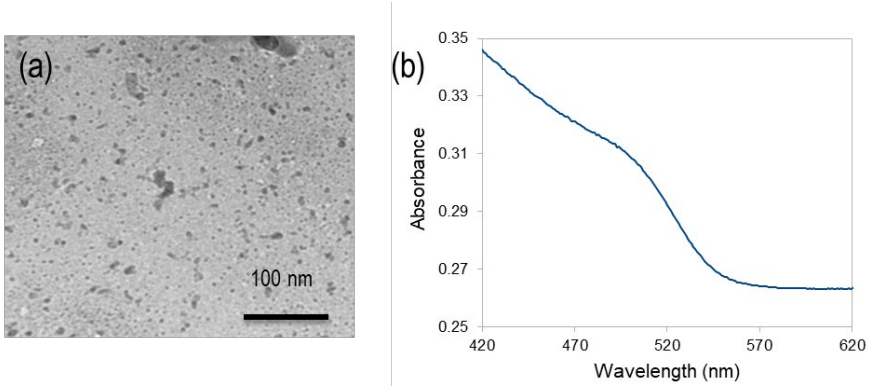

Figure 1. (a) Transmission electron micrograph of 5 nm diameter CdSe nanoparticles and (b) UV–vis spectrum. Scale bar = 100 nm.

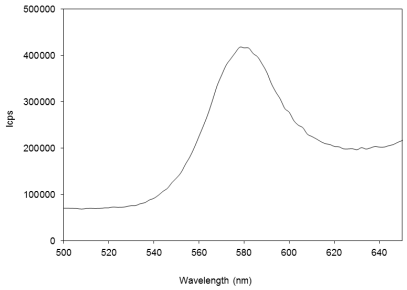

Figure 2. Emission spectra of CdSe nanoparticles excited at 355 nm.

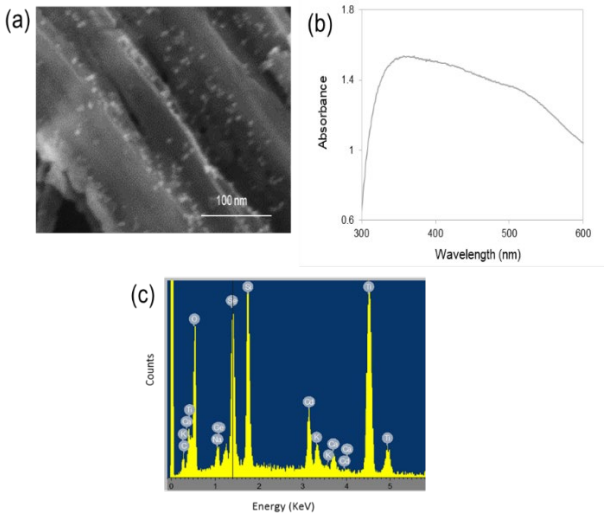

Figure 3. (a) Scanning electron micrograph, (b) UV–vis spectrum, and (c) EDS analysis of ordered arrays of CdSe-TiO_2 nanostructures.

Nanophotocatalysts have been evaluated for photocatalytic reduction of CO_2 with H_2O vapor by exposing three 1cm^2 of catalyst in ~20 cc gas mixture and under ambient light. The

amount of gases generated through prolonged light-soaking is quantified by gas-chromatography. A gas chromatographic analysis shows that the primary products are hydrogen, carbon monoxide along with methanol after several hours of exposure to sun light.

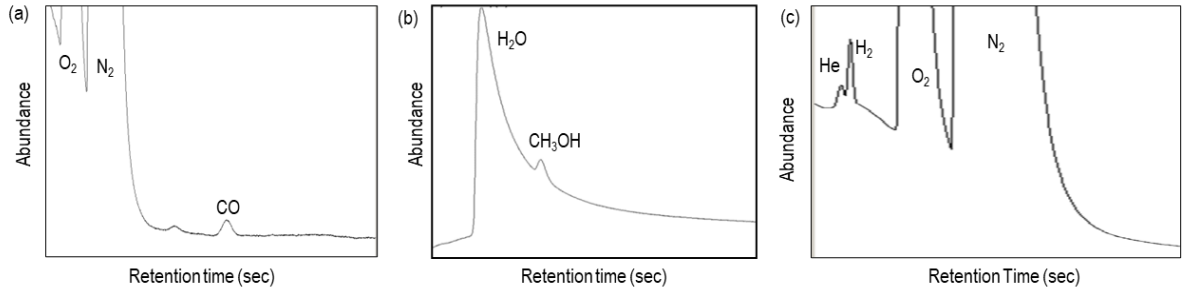

Figure 4. GC analysis showing carbon monoxide, methanol, and hydrogen produced after several hours of exposure to sun light evolution on CdSe-TiO_2 nanostructures. GC was equipped with OV1 and pora-plot columns. OV1 for monitoring methanol and the pora plot for all other gases including H_2 and CO.

Evolution of hydrocarbons after prolonged light exposure detected and quantified by GC shows that, as expected, a longer exposure (from 1, 4 to 8 hours) increases the amount of gases produced (data not shown). The amount and the type of gases produced are highly dependent upon nanophotocatalyst' composition.

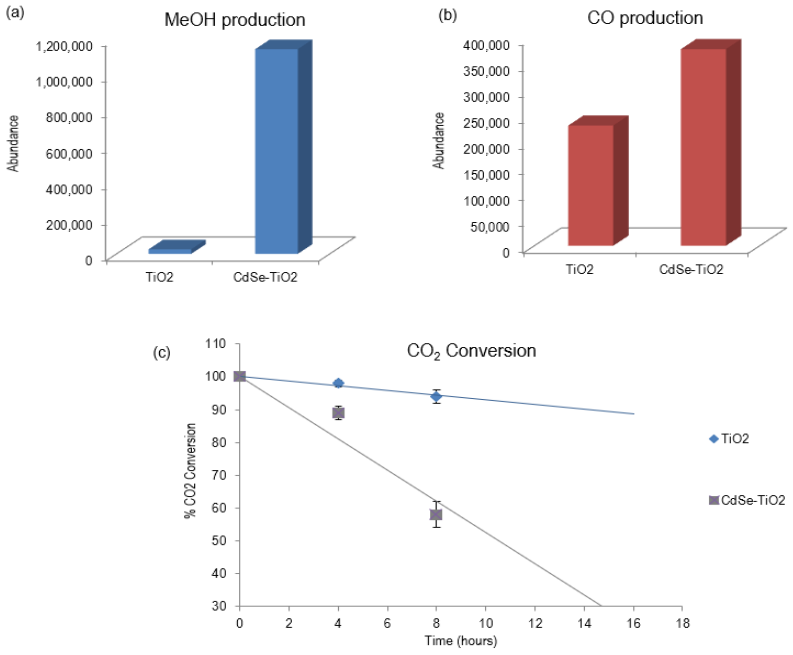

Figure 5. (a) Methanol production, (b) Carbon monoxide evolution after exposure of titania-based catalysts for 4 hours at 35ºC, and (c) time dependence studies of CO_2 conversion after prolonged exposure in sun light.

There are several major findings from the data collected. First, carbon monoxide production is higher when CdSe-TiO_2 is employed versus TiO_2 catalysts after four hours exposure under visible illumination at 35ºC (Figure 5). The yield of methanol is also significantly higher on

CdSe-TiO_2 when compared to TiO_2 nanorod catalyst array, approximatively 45 times higher. The amount of carbon monoxide produced is approximatively 40% higher when CdSe-TiO_2 catalyst is used in comparison with the titania. These results are in agreement with previous studies that suggest a higher efficiency in CO_2 photoreduction due to significantly increased lifetime of the charge-separated state. [10, 13, 16] Since the electron-hole recombination is two-three orders of magnitude faster than other electron-hole recombination any process that inhibits electron–hole recombination greatly increases the efficiency and rates of CO_2 photoreduction. Coupling the ordered TiO_2 nanorod arrays with CdSe nanoparticles increases spatial separation and diffusion lengths of photoexcited electrons and holes which result in increased CO_2 conversion. This indicates that the composition and ordered spatial arrangement of the TiO_2 surface is an extremely important factor in its catalytic activity. [14-17, 20]

Carbon dioxide evolution is also monitored during the CO_2/H_2O conversion (Figure 5c). The linear curve fitting indicates the conversion rate of CO_2, which is approximately 50% higher when using CdSe-TiO_2 sample as the photocatalyst. This is likely due to the coupling of pure TiO_2 with CdSe, which extends the adsorption of solar energy in the visible region and generates more electron-hole pairs, due to the smaller band gap of those sensitizers. In all cases, the highest gas yields are recorded when samples are exposed in sunlight at temperatures of 35^{o}C after prolonged sun illumination exposure. More experiments are underway to completely elucidate this phenomenon and will be reported at a later date.

Conclusions: We demonstrate solar conversion of carbon dioxide and water vapor to carbon monoxide, hydrogen and methanol by exposure of titania-based nanophotocatalysts to ambient light only. The photocatalytic performance of the nanoarchitectures developed here was highly dependent upon the nanoparticle's morphology, composition, illumination range, temperature and exposure time. The overall CO_2 conversion efficiency of quantum dot-titania nanostructures is significantly higher than that of pure TiO_2 nanorod array photocatalyst. The yield of methanol is approximatively 45 times higher while the amount of carbon monoxide produced is nearly 40% higher when CdSe-TiO_2 catalyst is used in comparison to TiO_2 under solar illumination. The improved conversion efficiency may result from the additional absorbance of visible light by CdSe quantum dots and the charge separation at the CdSe-TiO_2 interfaces. The conversion efficiency of this photocatalytic process remains to be improved for practical applications.

Acknowledgements: This work was supported by the Laboratory Directed Research and Development (LDRD) program within the Savannah River National Laboratory (SRNL). This work was produced by Battelle Savannah River Alliance, LLC under Contract No. 89303321CEM000080 with the U.S. Department of Energy. Publisher acknowledges the U.S. Government license to provide public access under the DOE Public Access Plan (http://energy.gov/downloads/doe-public-access-plan). We appreciate Y. Zhao's group for providing titania nanostructures.

References:

1. Ravanchi MT, Sahebdelfar S (2021) Catalytic conversions of CO2 to help mitigate climate change: Recent process developments, Process Safety and Environmental Protection 145:172–194.
2. Davis ST et. al. (2018) Net-zero emissions energy systems. Science, 360: eaas9793.
3. Hunyadi Murph SE, Lawrence K, Sessions H, Brown M, Larsen G (2020) Controlled Release of Hydrogen Isotopes from Hydride-Magnetic Nanomaterials, ACS Applied Materials & Interfaces, 12:9478-9488.

4. Hunyadi Murph SE, Sessions H, Lawrence K, Brown M, Ward, P (2021) Efficient Thermal Processes using Alternating Electromagnetic Field for Methodical and Selective Release of Hydrogen Isotopes, Energy and Fuels, 35: 3438-3448.
5. Ramseur JL (2019) U.S. Carbon Dioxide Emissions in the Electricity Sector: Factors, Trends, and Projections, Congressional Research Service, R45453.
6. Hunyadi Murph SE, Murph MA (2022) Nuclear fusion: the promise of endless energy, Physical Sciences Reviews,
7. Alcantara ML, Pacheco KA, Bresciani, AE, Alves RMB (2021) Thermodynamic Analysis of Carbon Dioxide Conversion Reactions. Case Studies: Formic Acid and Acetic Acid Synthesis Ind. Eng. Chem. Res. 60(25): 9246–9258
8. Hunyadi Murph SE, Larsen G., Coopersmith K. (2017) Anisotropic and shape-selective nanomaterials: structure-property relationships, nanostructure science and technology series. Springer Publisher, pp 1- 470.
9. Nguyen DLT, Kim Y, Hwang YJ, WDH.(2020) Progress in development of electrocatalyst for CO2 conversion to selective CO production Carbon Energy 2:72–98.
10. Lee YY, Jung HS, Kim JM, K YT (2018) Photocatalytic CO2 conversion on highly ordered mesoporous materials: Comparisons of metal oxides and compound semiconductors Applied Catalysis B: Environmental 224 :594–601.
11. Hunyadi Murph SE, Murphy CJ (2013) Patchy Silica-Coated Silver Nanowires as SERS Substrates. J. Nanoparticle Res. 15:1607.
12. Yu K P, Yu WY, Ku MC, Liou YC, Chien SH (2008) Pt/titania-nanotube: A potential catalyst for CO2 adsorption and hydrogenation Appl. Catal. B 84:112 -118.
13. Du K, Liu G, Chen X, Wang K (2018) Nanotube Heterostructures MoS2/CdS/TiO2 for CO2 Conversion ECS Trans. 85: 47
14. Hunyadi Murph, SE; Heroux, K, Turick, C, Thomas, D. (2012) Metallic and Hybrid Nanostructures: Fundamentals and Applications, in Applications of Nanomaterials, Series ISBN: 1-62699-000-X, Vol.4: Nanomaterials and Nanostructures, Volume (4), J.N. Govil, ISBN: 1-62699-004-2, Studium Press LLC, USA.
15. Hunyadi Murph SE (2020) Shape-Selective Mesoscale Nanoarchitectures: Preparation and Photocatalytic Performance, Catalysts, 10:532-552.
16. Kun, Y, Basnet, P, Sessions, H, Larsen, G.; Hunyadi Murph, SE, Zhao, Y (2016) Fe2O3/TiO2 Core-Shell Nanorod Array for Visible Light Photocatalysis" Catalysis Today, special issue C1 Catalytic Chemistry, 51-58.
17. He, Y, Basnet, P, Hunyadi Murph, SE, Zhao, Y (2013) Ag Nanoparticle Embedded TiO2 Composite Nanorod Arrays Fabricated by Oblique Angle Deposition: Toward Plasmonic Photocatalysis, ACS Applied Materials & Interfaces, 5: 11818-11827.
18. Wang Y, Tang, Z, Correa-Duarte MA, Pastoriza-Santos I, Giersig, M, Kotv NA, Liz-Marzan, L. (2004) Mechanism of Strong Luminescence Photoactivation of Citrate-Stabilized Water-Soluble Nanoparticles with CdSe Cores J. Phys. Chem. B, 108:15461-15469.
19. Mahtab R, Sealey SM, Hunyadi SE, Kinard B, Ray T, Murphy CJ (2007) Influence of the Nature of Quantum Dot Surface Cations on Interactions with DNA J. Inorg. Biochem., 101: 559-564
20. Hunyadi Murph, SE, Serkiz S, Fox E, Colon-Mercado H, Sexton L, Siegfried M (2011) Synthesis, Functionalization, Characterization and Application of Controlled Shape Nanoparticles in Energy Production, Fluorine-Related Nanoscience with Energy Applications, ACS Symposium Series, Volume 1064, Chapter 8, 127-163.